

# A MUSE study of the fast bar in the weakly-interacting galaxy NGC 4264

Virginia Cuomo<sup>1</sup> , Enrico Maria Corsini<sup>1,2</sup>, Alfonso J. L. Aguerri<sup>3,4</sup>  
and Victor P. Debattista<sup>5</sup>

<sup>1</sup>Dipartimento di Fisica e Astronomia “G. Galilei”, Università di Padova,  
vicolo dell’Osservatorio 3, I-35122 Padova, Italy  
email: [virginia.cuomo@phd.unipd.it](mailto:virginia.cuomo@phd.unipd.it)

<sup>2</sup>INAF - Osservatorio Astronomico di Padova,  
vicolo dell’Osservatorio 2, I-35122 Padova, Italy

<sup>3</sup>Instituto de Astrofísica de Canarias,  
calle Vía Láctea s/n, 38205 La Laguna, Tenerife, Spain

<sup>4</sup>Departamento de Astrofísica, Universidad de La Laguna,  
Avenida Astrofísico Francisco Sánchez s/n, 38206 La Laguna, Tenerife, Spain

<sup>5</sup>Jeremiah Horrocks Institute, University of Central Lancashire, PR1 2HE Preston, UK

**Abstract.** We present surface photometry and stellar kinematics of NGC 4264, a lenticular galaxy in the region of the Virgo Cluster undergoing a tidal interaction with its neighbour, NGC 4261. We measured the bar radius and strength from SDSS imaging and the bar pattern speed from MUSE integral-field spectroscopy. We find that NGC 4264 hosts a strong and large bar, which is rotating fast. The accurate measurement of the bar rotation rate allows us to exclude that the formation of the bar was triggered by the ongoing interaction.

**Keywords.** galaxies: evolution, galaxies: individual (NGC 4264), galaxies: interactions, galaxies: kinematics and dynamics

## 1. Introduction

The bar pattern speed  $\Omega_{\text{bar}}$  is the angular velocity of the bar rotating around the galactic centre. It can be parametrised through the bar rotation rate  $\mathcal{R}$ , which is defined as the ratio between the corotation radius  $R_{\text{cor}}$  and the length of the bar semi-major axis,  $a_{\text{bar}}$ . In turn,  $R_{\text{cor}}$  is measured as the ratio between the circular velocity  $V_{\text{circ}}$  of the galaxy and  $\Omega_{\text{bar}}$ . Bars with  $1.0 \leq \mathcal{R} \leq 1.4$  end close to their  $R_{\text{cor}}$  and are called *fast*, while bars with  $\mathcal{R} > 1.4$  are shorter than  $R_{\text{cor}}$  and are called *slow* (Athanassoula 1992; Debattista & Sellwood 2000). The value of  $\Omega_{\text{bar}}$  is expected to decrease with time because of the angular momentum exchange between the galaxy components and dynamical friction exerted on the bar by the dark matter (DM) halo. A huge amount of DM can efficiently slow down the rotation of the bar, which is expected to be *slow* (Debattista & Sellwood 1998; Athanassoula *et al.* 2013). The determination of  $\mathcal{R}$  allows both to investigate the secular evolution of barred galaxies and to put constraints on the DM distribution in their central regions.

The only direct way to recover  $\Omega_{\text{bar}}$  is to apply the model-independent Tremaine-Weinberg method (TW Tremaine & Weinberg 1984). It is based on the simple equation  $\Omega_{\text{bar}} \sin i = \langle V \rangle / \langle X \rangle$ , where  $\Omega_{\text{bar}}$  is given by the ratio of the luminosity-averaged position  $\langle X \rangle$  and line-of-sight (LOS) velocity  $\langle V \rangle$  of the stars. These quantities are measured along apertures crossing the bar and located parallel to the disc major axis, when its

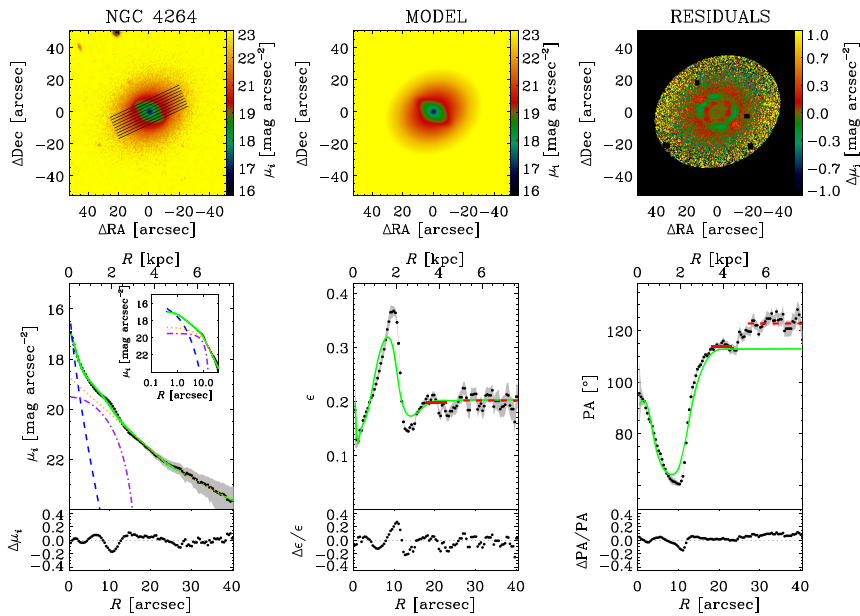


**Figure 1.** Photometric decomposition of NGC 4264. Upper panels: observed, modelled, and residual surface brightness distributions. The FOV is oriented with North up and East left. The apertures are shown as black lines in the observed image. Lower panels: radial profiles of surface brightness, PA, and ellipticity of the observed (black dots with gray error bars) and seeing-convolved modelled image (green solid line) and their difference. The surface brightness radial profiles of the best-fitting bulge (blue dashed line), bar (magenta dash-dotted line), and disc (orange dotted line) are shown for the semi-major axis distance to the galaxy centre. The red solid and dashed segments give the mean values of PA and ellipticity for the inner and outer portions of the disc, respectively.

inclination  $i$  is known. The resulting values are fitted with a line and the corresponding slope is proportional to  $\Omega_{\text{bar}}$ .

Despite its simple formulation, the method has some restrictions: undisturbed morphology and kinematics are required to correctly identify the disc position angle (PA) along which to locate the apertures, so interacting galaxies are generally avoided.

About 100 galaxies have been analysed with the TW method using long-slit (Corsini 2011) and integral-field spectroscopy (Debattista & Williams 2004; Aguerri *et al.* 2015; Guo *et al.* 2019; Cuomo *et al.* 2019a), hosting only *fast* bar. No trends were found between  $\mathcal{R}$  and Hubble type or DM content, but so far measurements have large uncertainties ( $\langle \Delta \Omega_{\text{bar}} / \Omega_{\text{bar}} \rangle = 0.3$ ,  $\langle \Delta \mathcal{R} / \mathcal{R} \rangle = 0.4$ ).

## 2. NGC 4264: an interacting galaxy

We analysed the case of NGC 4264, a lenticular galaxy in the region of the Virgo Cluster, with some hints of interaction. In fact, NGC 4264 is located close to the bright elliptical galaxy NGC 4261 at a projected distance of 30 kpc and they are probably gravitationally bound. We measured the surface photometry from the SDSS *i*-band images with the IRAF ELLIPSE task (Jedrzejewski 1987). We observed a twist in the outer disc isophotes. The PA radial profile (Fig. 1, bottom-right panel) shows two disc regions characterised by two constant PAs, which differ by  $\Delta \text{PA} \sim 10^\circ$ . This is confirmed by the photometric decomposition we performed using the GASP2D code (Méndez-Abreu *et al.* 2014), in which we included a double-exponential law (Méndez-Abreu *et al.* 2017) to describe the contribution of the disc to the galaxy surface brightness (Fig. 1).

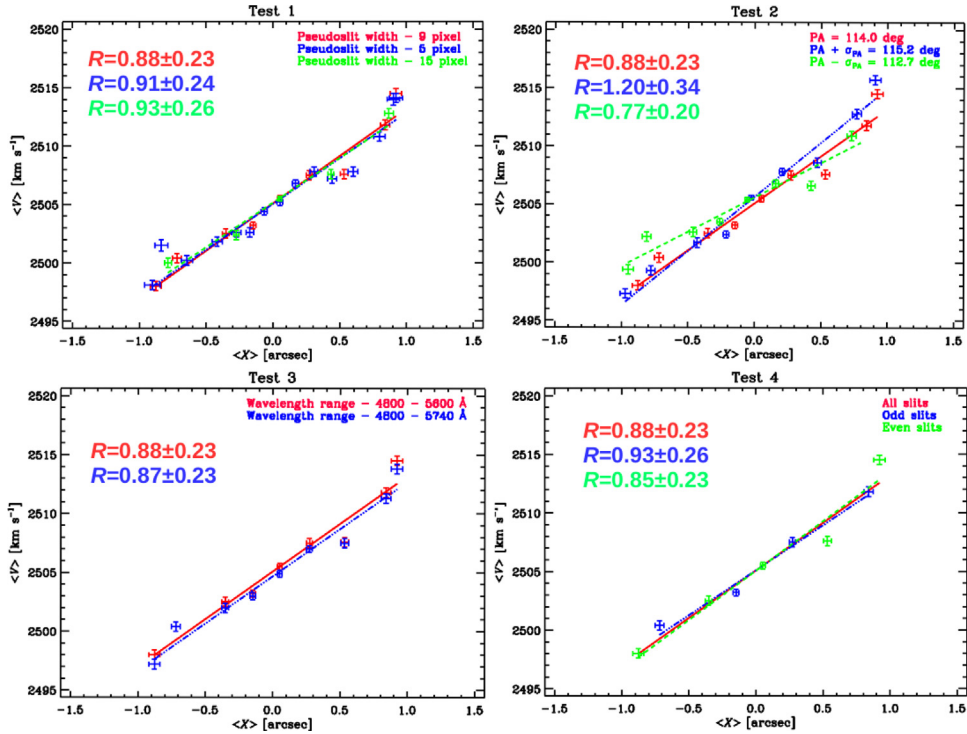


**Figure 2.** Pattern speed of the bar in NGC 4264 for the different tests performed to assess how the slope of the best-fitting straight line changes as a function of the aperture width (top left panel), PA (top right panel), wavelength range (bottom left panel), and number of apertures (bottom right panel). The reference value in each panel is given by the solid red line.

### 3. Characterising the bar

The correct determination of the disc PA is crucial for a solid measurement of  $\Omega_{\text{bar}}$  with the TW method (Debattista 2003; Zou *et al.* 1984). In order to deal with this problem in the case of an interacting galaxy, it is necessary to use the synergy between high-quality photometry and integral-field spectroscopy. The high spatial resolution of MUSE allowed us to define *a posteriori* the PA of the disc, and to fine-tune the number and length of the apertures used in the TW analysis.

To characterise the bar it is necessary to measure its radius  $a_{\text{bar}}$ , strength  $S_{\text{bar}}$ , and pattern speed  $\Omega_{\text{bar}}$ . We obtained  $a_{\text{bar}} = 3.2 \pm 0.5$  kpc by applying three different methods to the SDSS *i*-band image: the photometric decomposition (Fig. 1), Fourier analysis, and analysis of the PA of the deprojected isophotes. The Fourier analysis (Aguerri *et al.* 2000) allowed us also to derive  $S_{\text{bar}} = 0.31 \pm 0.04$ . Our results are consistent with typical values found for lenticular galaxies (Aguerri *et al.* 2009). Finally, we measured  $\Omega_{\text{bar}} = 71 \pm 4$  km s<sup>-1</sup> kpc<sup>-1</sup> with the TW method: we defined 9 apertures located parallel to the major axis of the inner disc. To recover the values of  $\langle X \rangle$  and  $\langle V \rangle$ , we collapsed the MUSE datacube between 4800 and 5600 Å in the spectral and spatial directions, respectively. In particular, we extracted the LOS velocity from the resulting spectra. We fitted with the IDL FITEXY task the resulting values (Fig. 2, red solid line).

To recover  $V_{\text{circ}} = 189 \pm 10$  km s<sup>-1</sup>, we measured the stellar kinematics from the entire MUSE datacube with PPF (Cappellari & Emsellem 2004) and GANDALF codes (Sarzi *et al.* 2006) on a Voronoi tessellation (Cappellari & Copin 2003), and we applied the

asymmetric drift correction, following the prescription of [Aguerri et al. \(2015\)](#). Finally, we derived  $R_{\text{cor}} = 2.8 \pm 0.2$  kpc, and  $\mathcal{R} = 0.88 \pm 0.23$ . This means NGC 4264 hosts a *fast* bar.

#### 4. Discussion and conclusions

We tested the stability of our results by verifying all the ingredients of the TW analysis. We varied width, number, and spectral range used to define the apertures and we found compatible results. On the contrary, changing the PA of the apertures led to different results (Fig. 2). In particular, the PA of the outer disc corresponds to  $\mathcal{R} < 1.0$ , which is unphysical. These tests confirm that the bar of NGC 4264 is living in the inner part of the disc, and that the correct identification of the PA of the disc is crucial for the TW method. All the details are given in [Cuomo et al. \(2019b\)](#).

This represents a pilot study for further accurate MUSE TW measurements: the values of  $\Omega_{\text{bar}}$  and  $\mathcal{R}$  for NGC 4264 are amongst the best-constrained ones ever obtained with the TW method ( $\Delta\Omega_{\text{bar}}/\Omega_{\text{bar}} = 0.06$ ,  $\Delta\mathcal{R}/\mathcal{R} = 0.26$ ).

These results allowed us to constrain the formation mechanism of the bar in NGC 4264. We interpreted the twist of the outer isophotes as suggestive of a warp due to the ongoing interaction with NGC 4261. Since the bar of NGC 4264 is *fast*, we concluded that its formation was not triggered by the recent interaction or by a previous interaction with an other galaxy, because this would form a *slow* bar ([Martinez-Valpuesta et al. 2017](#)).

Further accurate measurements of  $\Omega_{\text{bar}}$  and  $\mathcal{R}$  in a large number of barred galaxies would be of considerable interest to severely test the predictions of numerical simulations about the time evolution of  $a_{\text{bar}}$  and  $\Omega_{\text{bar}}$  as a function of gas content, luminous and DM distribution ([Athanassoula et al. 2013](#)).

#### References

- Aguerri, J. A. L., Muñoz-Tuñón, C., Varela, A. M., et al. 2000, *A&A*, 361, 841
- Aguerri, J. A. L., Méndez-Abreu, J., & Corsini, E. M. 2009, *A&A*, 495, 491
- Aguerri, J. A. L., Méndez-Abreu, J., Falcón-Barroso, J., et al. 2015, *A&A*, 576, A102
- Athanassoula, E. 1992, *MNRAS*, 259, 345
- Athanassoula, E., Machado, R. E. G., & Rodionov, S. A. 2013, *MNRAS*, 429, 1949
- Cappellari, M. & Copin, Y. 2003, *MNRAS*, 342, 345
- Cappellari, M. & Emsellem, E. 2004, *PASP*, 116, 138
- Corsini, E. M. 2011, Memorie della Societa Astronomica Italiana Supplementi, 18, 23
- Cuomo, V., Aguerri, J. A. L., Corsini, E. M., et al. 2019a, *A&A*, 632, A51, ([arXiv:1909.01023](#))
- Cuomo, V., Corsini, E. M., Aguerri, J. A. L., et al. 2019b, *MNRAS*, 488, 4972
- Debattista, V. P. & Sellwood, J. A. 1998, *ApJl*, 493, L5
- Debattista, V. P. & Sellwood, J. A. 2000, *ApJ*, 543, 704
- Debattista, V. P. & Williams, T. B. 2004, *ApJ*, 605, 714
- Sarzi, M., Falcón-Barroso, J., Davies, R. L., et al. 2006, *MNRAS*, 366, 1151
- Debattista, V. P. 2003, *MNRAS*, 342, 1194
- Martinez-Valpuesta, I., Aguerri, J. A. L., González-García, A. C., et al. 2017, *MNRAS*, 464, 1502
- Méndez-Abreu, J., Debattista, V. P., Corsini, E. M., et al. 2014, *A&A*, 572, A25
- Méndez-Abreu, J., Ruiz-Lara, T., Sánchez-Menguiano, L., et al. 2017, *A&A*, 598, A32
- Guo, R., Mao, S., Athanassoula, E., et al. 2019, *MNRAS*, 482, 1733
- Jedrzejewski, R. I. 1987, *MNRAS*, 226, 747
- Tremaine, S. & Weinberg, M. D. 1984, *ApJl*, 282, L5
- Zou, Y., Shen, J., Bureau, M., et al. 2019, *ApJ*, 884, 23